TECHNISCHE MECHANIK, Band 22, Heft 3, (2002), 235-243
Manuskripteingang: 17. August 2001

A Finite Element Procedure for Three-dimensional Analyses of Thermopiezoelectric Structures in Static Applications

Fulin Shang, M. Kuna, M. Scherzer

The development and application of smart structures and smart composite materials require efficient numerical tools to evaluate the thermopiezoelectric behavior and stress state. In this paper, finite element techniques are suggested for three-dimensional coupled thermo-electromechanical static analyses. The actual thermo-piezoelectric responses subjected to thermal loadings can be determined by adopting a procedure TPESAP. The detailed implementation is presented with emphasis on the integration with software ABAQUS. Several verification example problems are discussed, including the benchmark problem of a five-layer hybrid plate.

1 Introduction

With the growing application of smart material systems in innovative technical areas, the analysis of piezoelectric elements has received considerable attention in recent years. Thermal effects have been demonstrated to be crucial in several applications, see for examples Hilczer and Malecki (1986), Rao and Sun (1994), Tzou and Tseng (1990). It has also been recognized that thermally induced deformation/stress is an essential consideration in the distributed sensing and control of laminated structures with integrated piezoelectric actuators or sensors. Thermal effects, such as, temperature-induced deformation effect and pyroelectric effect, are especially important for many smart ceramic materials. As a result, it may be impossible to predict the electromechanical behavior without considering these effects.

Several finite element formulations of thermopiezoelectric materials have been developed, taking into account the thermal effects for different purposes, such as precision control of piezoelectric laminates subject to a steady-state temperature field (Tzou and Ye, 1994), distributed dynamic measurement and active vibration control of intelligent structures (Tzou and Tseng, 1990). A weak form of finite element formulations of fully coupled thermopiezoelectricity has been presented for determining the static and dynamic responses under combined thermal, electric and mechanical excitation (Görnandt and Gabbert, 2000).

These efforts seem to be strenuous, especially when noting that great benefit could be provided by commercial finite element analysis software. For instance, efficient numerical tools for fracture mechanics analysis have been supplied by some of commercial software. Therefore, it would be a wiser choice to develop only pre- or post-processing procedures based on them, when analyzing the crack problems of thermo-piezoelectric materials. The starting point of this work is to follow the above approach.

A three-dimensional (3D) formulation of thermopiezoelectric problems is presented for general purpose, making use of the weak form of thermo-electromechanical equilibrium. The detailed numerical implementation is outlined with emphasis on the integration with commercial software ABAQUS. Verification examples are discussed afterwards, including a benchmark problem.

2 Finite Element Formulation of Thermopiezoelectricity

The constitutive relations for a thermopiezoelectric continuum are given by

$$\begin{aligned} \sigma_{ij} &= c_{ijkl}\varepsilon_{kl} - e_{kij}E_k - \lambda_{ij}\theta \\ D_i &= e_{ijk}\varepsilon_{jk} + \in_{ij} E_j + p_i\theta \end{aligned} \tag{1}$$

where $c_{ijkl}, e_{kij}, \lambda_{ij}, \in_{ij}, p_i$ are the elastic constants, piezoelectric modules, temperature stress coefficients, dielectric constants, pyroelectric constants, respectively; $\sigma_{ij}, \varepsilon_{ij}, D_i, E_i$ denote the stress, strain, electric displacement, and electric field, respectively; θ is the temperature change.

The governing equations for thermopiezoelectricity include three fundamental equations: (1) the equations of stress equilibrium, (2) the equation of the quasi stationary electric field, and (3) the heat conduction equation. For a stationary case, the system of differential equations is given by

$$\sigma_{ij,j} = 0 \qquad D_{i,i} = 0 \qquad \kappa_{ij}\theta_{,ij} = 0 \tag{2}$$

where κ_{ij} are the heat conduction coefficients. A complete description of the field problem includes mechanical, electric and thermal boundary conditions as well, prescribed at corresponding parts of the boundary S

$$\begin{aligned} &u_i = \bar{u}_i \ \ on \ \ S_u \qquad \sigma_{ij}n_j = \bar{t}_i \ \ on \ \ S_\sigma \\ &\varphi = \bar{\varphi} \ \ on \ \ S_\varphi \qquad D_i n_i = -\bar{Q} \ \ on \ \ S_D \\ &\theta = \bar{\theta} \ \ on \ \ S_\theta \qquad \kappa_{ij}\theta_{,j}n_i = \bar{q}_s \ \ on \ \ S_{qs} \\ &-\kappa_{ij}\theta_{,j}n_i = \bar{q}_h = h_v(\theta + \Theta_0 - \Theta_\infty) \ \ on \ \ S_{qh} \end{aligned} \tag{3}$$

where u_i is the mechanical displacement vector, φ is the scalar electric potential, n_i is the direction cosine component, $(\bar{})$ denotes a prescribed value, h_v is the convective heat transfer coefficient, $\bar{q}_s$ and $\bar{q}_h$ mean heat fluxes, Θ_0 is a stress free reference temperature and Θ_∞ is the environmental temperature.

Adopting the weak form of the thermo-electromechanical equilibrium developed by Görnandt and Gabbert (2000), an appropriate formulation of finite element method (FEM) is developed below based upon ABAQUS 20-node quadratic brick piezoelectric elements C3D20E.

By assuming the shape functions $\mathbf{N_u}, \mathbf{N}_\varphi, \mathbf{N}_\theta$, all independent field variables $\mathbf{u_e}, \varphi_\mathbf{e}, \boldsymbol{\theta}_\mathbf{e}$ within a finite element (subscript e) can be defined as

$$\begin{aligned} &\mathbf{u_e} = \mathbf{N_u u_k} \qquad \varphi_\mathbf{e} = \mathbf{N}_\varphi \boldsymbol{\varphi}_\mathbf{k} \qquad \boldsymbol{\theta}_\mathbf{e} = \mathbf{N}_\theta \boldsymbol{\theta}_\mathbf{k} \\ &\boldsymbol{\varepsilon}_\mathbf{e} = \mathbf{B_u u_k} \qquad \mathbf{E_e} = -\mathbf{B}_\varphi \boldsymbol{\varphi}_\mathbf{k} \qquad \mathbf{g_e} = -\mathbf{B}_\theta \boldsymbol{\theta}_\mathbf{k} \end{aligned} \tag{4}$$

where $\mathbf{u_k}, \boldsymbol{\varphi}_\mathbf{k}, \boldsymbol{\theta}_\mathbf{k}$ are the unknown nodal displacement vector, nodal electric potential vector, and nodal temperature vector, respectively; $\mathbf{g_e}$ denotes the temperature gradient vector. $\mathbf{B_u} = \mathbf{L_u N_u}$, $\mathbf{B}_\varphi = \mathbf{L}_\varphi \mathbf{N}_\varphi$, $\mathbf{B}_\theta = \mathbf{L}_\theta \mathbf{N}_\theta$ and the symbols $\mathbf{L_u}, \mathbf{L}_\varphi, \mathbf{L}_\theta$ are the differential operators with respect to a global Cartesian coordinates x, y, z as

$$\begin{aligned} \mathbf{L}_\mathbf{u}^\mathbf{T} &= \begin{bmatrix} \partial/\partial x & 0 & 0 & \partial/\partial y & 0 & \partial/\partial z \\ 0 & \partial/\partial y & 0 & \partial/\partial x & \partial/\partial z & 0 \\ 0 & 0 & \partial/\partial z & 0 & \partial/\partial y & \partial/\partial x \end{bmatrix} \\ \mathbf{L}_\varphi^\mathbf{T} &= \mathbf{L}_\theta^\mathbf{T} = \{\partial/\partial x \quad \partial/\partial y \quad \partial/\partial z\} \end{aligned} \tag{5}$$

Specifically, for the elements C3D20E, we have

$$\mathbf{u}_\mathbf{e}^\mathbf{T} = \{u_x \quad u_y \quad u_z\}_e \tag{6}$$

$$\mathbf{u}_\mathbf{k}^\mathbf{T} = \{u_{x1} \quad u_{y1} \quad u_{z1} \quad u_{x2} \quad u_{y2} \quad u_{z2} \quad . \ . \ . \quad u_{x20} \quad u_{y20} \quad u_{z20}\}_e \tag{7}$$

$$\boldsymbol{\varphi}_\mathbf{k}^\mathbf{T} = \{\varphi_1 \quad \varphi_2 \quad \ldots \quad \varphi_{20}\}_e \tag{8}$$

$$\boldsymbol{\theta}_\mathbf{k}^\mathbf{T} = \{\theta_1 \quad \theta_2 \quad \ldots \quad \theta_{20}\}_e \tag{9}$$

where $u_{xi}, u_{yi}, u_{zi}, \varphi_i, \theta_i$ are the nodal unknowns of node i (=1 to 20) of the element e, and the superscript **T** denotes the matrix/vector transpose.

Then, the finite element approximation of the differential equations for each element can be obtained as

$$\begin{aligned}
&\mathbf{K}^{e}_{uu}\mathbf{u}_k+\mathbf{K}^{e}_{u\varphi}\varphi_k-\mathbf{K}^{e}_{u\theta}\theta_k=\mathbf{f}^{e}_{u}\\
&\mathbf{K}^{e}_{\varphi u}\mathbf{u}_k-\mathbf{K}^{e}_{\varphi\varphi}\varphi_k+\mathbf{K}^{e}_{\varphi\theta}\theta_k=\mathbf{f}^{e}_{\varphi}\\
&\mathbf{K}^{e}_{\theta\theta}\theta_k=\mathbf{f}^{e}_{\theta}
\end{aligned}\tag{10}$$

The element matrices and vectors are

$$\begin{aligned}
&\mathbf{K}^{e}_{uu}=\int_{V^e}\mathbf{B}_u^{T}\mathbf{c}\mathbf{B}_u dV^e \qquad \mathbf{K}^{e}_{u\varphi}=\int_{V^e}\mathbf{B}_u^{T}\mathbf{e}\mathbf{B}_\varphi dV^e \qquad \mathbf{K}^{e}_{u\theta}=\int_{V^e}\mathbf{B}_u^{T}\boldsymbol{\lambda}\mathbf{N}_\theta dV^e\\
&\mathbf{K}^{e}_{\varphi u}=\int_{V^e}\mathbf{B}_\varphi^{T}\mathbf{e}^{T}\mathbf{B}_u dV^e \qquad \mathbf{K}^{e}_{\varphi\varphi}=\int_{V^e}\mathbf{B}_\varphi^{T}\in\mathbf{B}_\varphi dV^e \qquad \mathbf{K}^{e}_{\varphi\theta}=\int_{V^e}\mathbf{B}_\varphi^{T}\mathbf{p}\mathbf{N}_\theta dV^e\\
&\mathbf{K}^{e}_{\theta\theta}=\int_{V^e}\mathbf{B}_\theta^{T}\boldsymbol{\kappa}^{T}\mathbf{B}_\theta dV^e \qquad \mathbf{f}^{e}_{u}=\int_{V^e}\mathbf{N}_u^{T}\mathbf{f}_b dV^e+\int_{S_\sigma}\mathbf{N}_u^{T}\mathbf{f}_s dS_\sigma+\mathbf{N}_u^{T}\mathbf{f}_c\\
&\mathbf{f}^{e}_{\varphi}=-\int_{S_D}\mathbf{N}_\varphi^{T}\mathbf{Q}_s dS_D \qquad \mathbf{f}^{e}_{\theta}=\int_{S_{qs}}\mathbf{N}_\theta^{T}\mathbf{q}_s dS_{qs}+\int_{S_{qh}}\mathbf{N}_\theta^{T}\mathbf{h}_v(\Theta_\infty-\Theta)dS_{qh}
\end{aligned}\tag{11}$$

Assembling all the element matrices, the global system equations are derived as

$$\begin{bmatrix}\mathbf{K}_{uu} & \mathbf{K}_{u\varphi} & -\mathbf{K}_{u\theta}\\ \mathbf{K}_{\varphi u} & -\mathbf{K}_{\varphi\varphi} & \mathbf{K}_{\varphi\theta}\\ \mathbf{0} & \mathbf{0} & \mathbf{K}_{\theta\theta}\end{bmatrix}\begin{Bmatrix}\mathbf{u}\\ \varphi\\ \theta\end{Bmatrix}=\begin{Bmatrix}\mathbf{f}_u\\ \mathbf{f}_\varphi\\ \mathbf{f}_\theta\end{Bmatrix}\tag{12}$$

One can see from equation (12) that the temperature field could be evaluated firstly and separately under a given thermal excitation, as

$$\mathbf{K}_{\theta\theta}\theta=\mathbf{f}_\theta\tag{13}$$

As a second step, the piezoelectric response under combined mechanical, electric and thermal loadings can be determined by solving the following equations

$$\begin{bmatrix}\mathbf{K}_{uu} & \mathbf{K}_{u\varphi}\\ \mathbf{K}_{\varphi u} & -\mathbf{K}_{\varphi\varphi}\end{bmatrix}\begin{Bmatrix}\mathbf{u}\\ \varphi\end{Bmatrix}=\begin{Bmatrix}\mathbf{f}_u+\mathbf{K}_{u\theta}\theta\\ \mathbf{f}_\varphi-\mathbf{K}_{\varphi\theta}\theta\end{Bmatrix}=\begin{Bmatrix}\mathbf{f}'_u\\ \mathbf{f}'_\varphi\end{Bmatrix}\tag{14}$$

In equation (14), $\mathbf{f}'_u,\mathbf{f}'_\varphi$ are defined as the generalized external mechanical and electric forces, which include the influence of temperature stress effect and pyroelectric effects, respectively.

3 The Detailed Implementation of Programming

The programming implementation based upon ABAQUS is presented in this section. Recalling that ABAQUS provides the capabilities of piezoelectric analysis and thermal analysis, i.e. the static response under combined mechanical and electric loading as well as temperature field under thermal conditions can be determined. To obtain the thermopiezoelectric response under thermal excitations, we need only insert the influence of temperature field into the standard modular of ABAQUS as external forces, as indicated in equation (14).

An example of implementation is illustrated using Gaussian numerical integration scheme of $3\times3\times3$ order. The element matrices in equation (14) can be evaluated as

$$\begin{aligned}
&\mathbf{K}^{e}_{u\theta}=\int_{V^e}\mathbf{B}_u^{T}\boldsymbol{\lambda}\mathbf{N}_\theta dV=\sum_{i=R_1}^{R_3}\sum_{j=S_1}^{S_3}\sum_{k=T_1}^{T_3}\left(\mathbf{B}_u^{T}\boldsymbol{\lambda}\mathbf{N}_\theta\det[\mathbf{J}]\big|_{(i,j,k)}w_i w_j w_k\right)\\
&\mathbf{K}^{e}_{\varphi\theta}=\int_{V^e}\mathbf{B}_\varphi^{T}\mathbf{p}\mathbf{N}_\theta dV=\sum_{i=R_1}^{R_3}\sum_{j=S_1}^{S_3}\sum_{k=T_1}^{T_3}\left(\mathbf{B}_\varphi^{T}\mathbf{p}\mathbf{N}_\theta\det[\mathbf{J}]\big|_{(i,j,k)}w_i w_j w_k\right)
\end{aligned}\tag{15}$$

where R_i, S_i, T_i and w_i (i = 1, 2, 3) are the location of integration points and the weights, and $\det[\mathbf{J}]$ is the determinant of the Jacobian matrix.

Secondly, the matrices $\mathbf{K}^{e}_{u\theta}$ and $\mathbf{K}^{e}_{\varphi\theta}$ of each element are assembled into global system matrices as

$$\begin{aligned} \mathbf{K}_{u\theta} &= \sum_{e} \mathbf{K}^{e}_{u\theta} \\ \mathbf{K}_{\varphi\theta} &= \sum_{e} \mathbf{K}^{e}_{\varphi\theta} \end{aligned} \tag{16}$$

Finally, multiplying these two global matrices by the nodal temperature field yields the external forces due to thermal effects as

$$\begin{aligned} \mathbf{f}^{'}_{u} &= \mathbf{K}_{u\theta}\boldsymbol{\theta} \\ \mathbf{f}^{'}_{\varphi} &= \mathbf{K}_{\varphi\theta}\boldsymbol{\theta} \end{aligned} \tag{17}$$

where the nodal temperature field is the standard output of ABAQUS heat analysis. The calculated nodal external forces can be inserted into ABAQUS as a standard input. A complete description of the integration aspects with ABAQUS Version 5.8 is outlined here. A procedure TPESAP (ThermoPiezoElectric Static Analysis Program) is developed for this purpose, which comprises the following six steps:

Step 1. Perform ABAQUS heat transfer analysis and output the temperature field at nodal points and at Gaussian integration points.

Step 2. Read the nodal data from Step 1 results file by utilizing ABAQUS/Make execution procedure. ABAQUS results file is written as a sequential file, and each record has regular format that can be accessed with the utility routines. Due to this excellent feature, user-written postprocessing programs can be compiled to use the analysis results file for specific purposes.

Step 3. Calculate the additional external forces in equation (17)

Step 4. Perform the piezoelectric analysis. The piezoelectric elements without thermal options are used. The calculated forces in Step 3 are included into the ABAQUS input file as concentrated mechanical and electric forces. Specifically, we use the input commands *CLOAD and *CECHARGE to prescribe concentrated nodal mechanical forces and electric charges, respectively. The output variables are displacements, electric potential, stresses, and electric displacements at Gaussian integration points.

Step 5. Calculate the thermopiezoelectric responses. The results of displacements and electric potential in Step 4 are the actual responses under thermal excitations. However, the stresses and electric displacements are not correct because of the piezoelectric constitutive relations assumed by ABAQUS. Therefore, these values should be determined from the real constitutive equation of thermopiezoelectricity, i.e. equation (1). To this end, the results files obtained in Step 1 and Step 4 are postprocessed by using ABAQUS/Make procedure. The actual thermopiezoelectric responses of the considered FEM model are determined.

Step 6. Perform a second piezoelectric analysis. This step serves for verification purpose. The results of stresses and electric displacements for the same model as that in step 4 but with thermal options are outputted. The thermal options include: (1) thermal expansion coefficients of materials, (2) initial temperature field of stress free state, and (3) current temperature field, which was derived in Step 1.

To achieve a higher numerical precision, the values of output variables at Gaussian integration points are utilized. However, the nodal averaged values can also be evaluated provided that the related result files are written in the required format.

4 Verification Examples

4.1 General Verifications

ABAQUS provides the capabilities of piezoelectric analysis and regular piezoelectric elements with thermal options, but without pyroelectric consideration. Therefore, the procedure presented in this work can be verified by ABAQUS to some extent in general. As explained in Section 3, the results of thermal stresses from Step 5 and Step 6 should be identical for any cases. However, the electric responses cannot be checked in the same manner. This will be illustrated by two examples, specifically.

a) One-element model

A one-element model is considered, where all degrees of freedom (u_x, u_y, u_z, φ) are constrained. The model is instantaneously heated up to 100°C from initial temperature 0°C. Due to the strong constraint, thermal stresses and electric displacements are induced. The numerical results of thermal stresses and electric displacements are found to be identical to the analytical solution, which is known for this special example problem.

Moreover, the results of electric displacements confirm that ABAQUS is unable to deal with pyroelectric effects. Hence, the postprocessing in Step 5 is necessary to determine the actual thermopiezoelectric responses.

b) Multi-element model

A multi-element model of a cube with partial constraints is developed as a second general test. Firstly, the model is subjected to a linear temperature field. But, under the selected constraints of degrees of freedom, a non-zero piezoelectric response is introduced. Secondly, an arbitrary temperature field is applied to this model. The numerical results of both considered problems show that thermal stresses can be computed correctly.

4.2 A Benchmark Example

A benchmark problem was proposed by Tauchert (1997) for assessing the validity of the plate-theory solution for piezothermoelastic behavior of hybrid laminates. The displacement and stress distributions of a five-layer plate subject to specified thermal loading, using the higher-order and classical bending theories, were compared. This problem has been investigated numerically by Görnandt and Gabbert (2000) and the electric potential and temperature distributions were presented there. Based upon these results, the procedure proposed in this work can be examined.

The laminate shown in Figure 1 consists of an isotropic middle layer, two adjacent orthotropic layers (0° and 90° ply-angles) and piezoelectric outer layers. Material properties of each layer used by both investigations are listed in Table 1. Here, $\alpha_{ij} = c^{-1}_{ijkl}\,\lambda_{kl}$ denotes the coefficients of linear thermal expansion. The five-layer plate has a length-to-thickness ratio of b/t = 5, each layer is of thickness $0.2t$. The laminate is subjected to a sudden sinusoidal temperature rise $\theta = \theta_0 \sin(\pi y / b)$ on the surface $z = -t/2$, while the temperature at the ends (y = 0, b) and on the surface $z = t/2$ were assumed to be constant at 0°C.

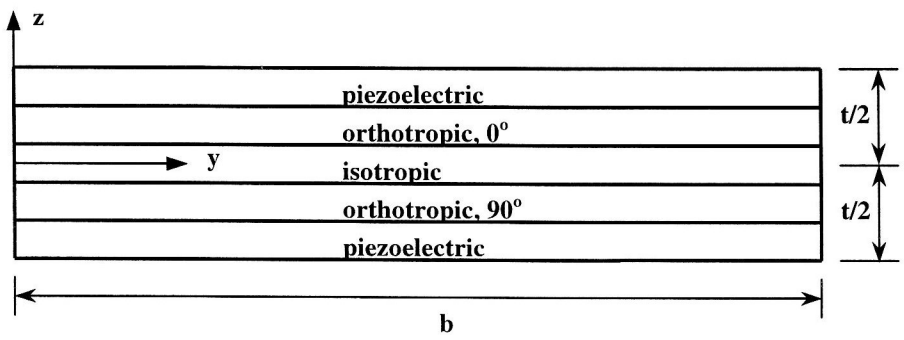

Figure 1. Laminate Configuration of the Benchmark Problem

The plate is simply supported at its ends and bounded in the x-direction along its edges to impose plane strain conditions. The electric potential at the ends of the piezoelectric layers as well as at the inner surfaces were taken to be zero, whereas arbitrary distribution of electric potential could occur on the outer surfaces.

Table 1. Material Properties (Görnandt (2001))

isotropic layer:	$E = E_0,\ \nu = \nu_0,\ \alpha = \alpha_0,\ \kappa = \kappa_0$
orthotropic layer, 90°:	$E_1 = 90E_0,\ E_2 = E_3 = 5E_0,\ G_{12} = G_{13} = 4E_0,\ G_{23} = 1.5E_0$
	$\nu_{12} = \nu_{13} = \nu_{23} = \nu_0,\ \alpha_1 = 0.0002\alpha_0,\ \alpha_2 = \alpha_3 = 0.2\alpha_0$
	$\kappa_{11} = 100\kappa_0,\ \kappa_{22} = \kappa_{33} = \kappa_0$
piezoelectric layer:	$E = E_0,\ \nu = \nu_0,\ \alpha = \alpha_0,\ \kappa = \kappa_0,\ \in_{11} = \in_{22} = \in_0,\ \in_{33} = 10\in_0$
	$p_3 = p_0,\ d_{31} = d_{32} = d_{24} = d_0,\ d_{33} = 1.4d_0$

Reference values of material constants selected for computations:

$E_0 = 2000\text{Nmm}^{-2},\ \nu_0 = 0.25,\ \alpha_0 = 10^{-5}\text{K}^{-1},\ \kappa_0 = 1.0\,\text{WK}^{-1}\text{m}^{-1}$

$\in_0 = 10^{-8}\,\text{Fm}^{-1},\ d_0 = 2\times10^{-10}\,\text{mV}^{-1},\ p_0 = 0.25\times10^{-3}\,\text{Cm}^{-2}\text{K}^{-1}$

The plate with length $b = 50\text{mm}$ and thickness $t = 10\text{mm}$ was discretized with $20\times10\times1$ C3D20E elements. At first, the steady-state temperature distribution was obtained. As shown in Figure 2, the present numerical results agree very well to those by Görnandt and Gabbert (2000), Görnandt (2001), and the analytical solution by Tauchert (1997) (which is labeled as 'Magdeburg' in the figure.).

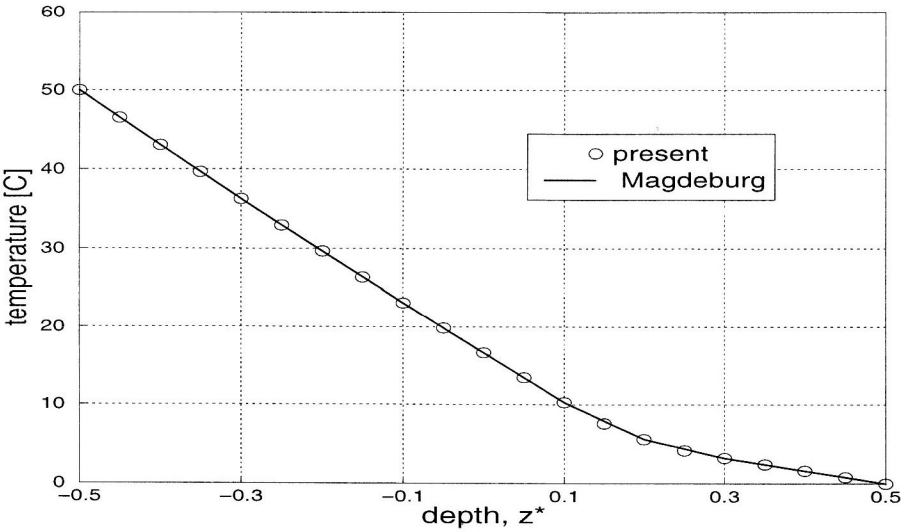

Figure 2. The Steady-State Temperature Distribution at $[0.5b, z^*]$

Secondly, thermopiezoelectric analyses were performed including the derived external forces. The distribution of the non-dimensional displacement ($w^* = wt/\alpha_0\theta_0 b^2$) in the thickness direction ($z^* = z/t$) at the center section of the plate ($y^* = y/b = 0.5$) is shown in Figure 3. The analytical solution developed by Tauchert (1997) neglected piezoelectric effects and pyroelectric effects, thus is an uncoupled one. The numerical solutions for this case were obtained in Görnandt and Gabbert (2000) ('uncoupled, Magdeburg'), and by the present procedure ('uncoupled, present'). Comparison of these results revealed a very good agreement. A comparison of coupled results, which include both piezoelectric effects and pyroelectric effects, is shown in Figure 3. The coupled results by the present procedure are rather close to those by Görnandt and Gabbert (2000). From a point of view of numerical approximation, these two predictions agree well. Further comparisons of coupled solutions and uncoupled solutions revealed the importance of considering thermal effects when determining thermo-piezoelectric responses.

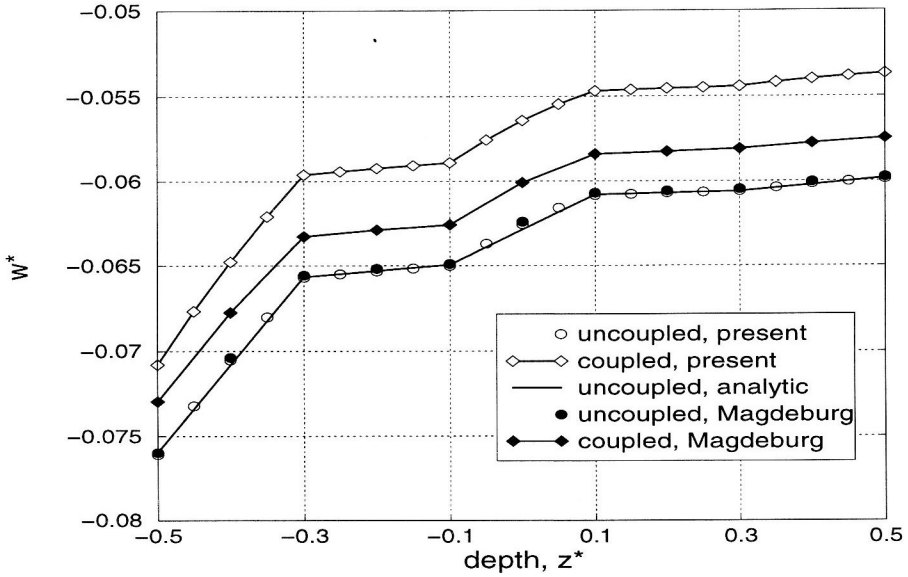

Figure 3. Non-dimensional Transverse Deflection $w^*[0.5b, z^*]$

The calculated induced electric potential over the lower piezoelectric layer is shown in Figure 4, where three piezoelectric analysis results (the dash line, circle symbols) were derived by including piezoelectric effect but neglecting pyroelectric effect, and two thermo-piezoelectric analysis results (the solid lines) by including both piezoelectric effect and pyroelectric effect. The standard ABAQUS piezoelectric analysis results agree exactly with the present piezoelectric results (open circles), while the results by Görnandt and Gabbert (2000) (filled circles) agree with them as well except the converse sign. The reason might be that a different polarization direction had been used in Görnandt and Gabbert (2000) and that the zero potential was not unambiguously fixed in Tauchert (1997). To verify the present numerical procedure, the electric potential difference between the thermopiezoelectric and piezoelectric analysis results are re-plotted in Figure 5. The excellent agreement implied the validity of the present procedure. Moreover, the big difference between thermopiezoelectric and piezoelectric analysis results indicate that the inclusion of pyroelectric effect is extremely important when evaluating the behavior of thermopiezoelectric structures.

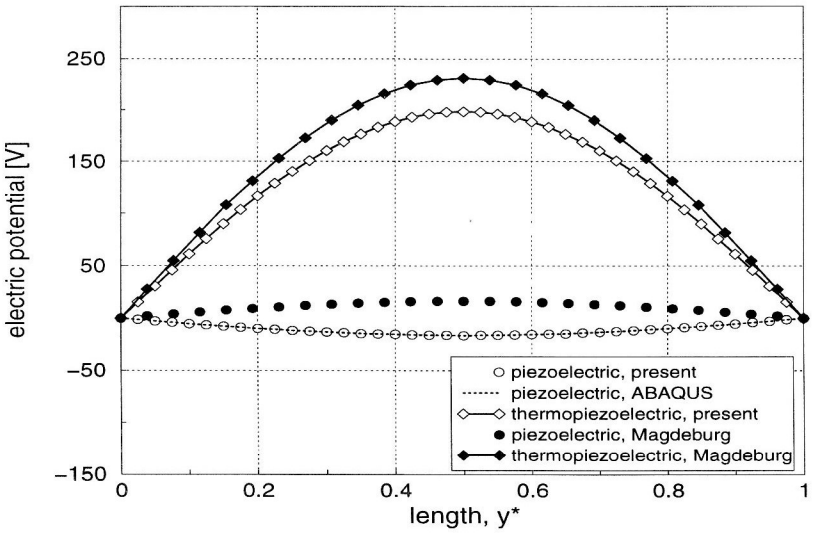

Figure 4. The electric potential at $[y^*, -0.5t]$

One can see from the above verifications that the procedure TPESAP is well suited and accurate for determining the static response of thermopiezoelectric structures. The procedure is quite general and can be used for various other piezoelectric problems. For illustration purpose, a steady-state heat transfer analysis was conducted here. However, a transient heat analysis and the subsequent thermopiezoelectric analysis, which have been calculated and checked in Görnandt and Gabbert (2000), can be performed in a similar manner.

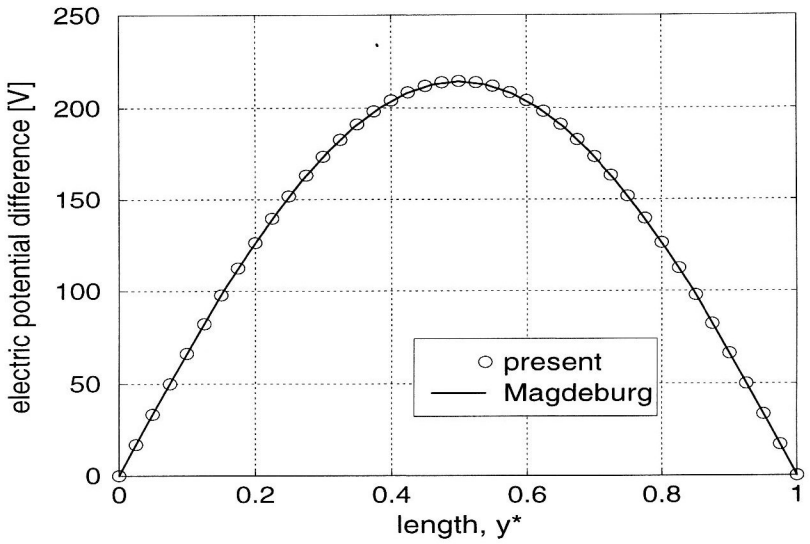

Figure 5. Electric potential difference between thermopiezoelectric and piezoelectric analyses at $[y^*,-0.5t]$

5 Concluding Remarks

The development and application of smart structures and smart composite materials require efficient numerical tools to evaluate the thermopiezoelectric behavior and stress state. Without loss of benefit provided by commercial analysis software, a finite element procedure is developed based on ABAQUS in this work. The actual thermopiezoelectric responses of three-dimensional structures subjected to thermal loadings can be determined by adopting the proposed procedure TPESAP. Its capability has been demonstrated by various verification problems. The numerical results for the benchmark problem of a five-layer hybrid plate, which was proposed by Tauchert (1997) as a yardstick for assessing the thermopiezoelectric analysis, are discussed extensively. The efficiency and accuracy of this procedure are proved to analyze thermopiezoelectric problems. Thus, many complicated problems of thermo-piezoelectric structures may be addressed. The advantages of this procedure have been demonstrated for 3D crack analyses of thermopiezoelectric materials, see Shang (2001). Moreover, the benchmark example confirmed that the pyroelectric effect could have a significant influence on the thermopiezoelectric behavior of piezoelectric structures.

Acknowledgments

The support from the Alexander von Humboldt Foundation of Germany is gratefully acknowledged.

Literature

1. Görnandt, A.; Gabbert, U.: Finite element analysis of thermopiezoelectric smart structures. Acta Mechanica, 154, (2002), 129-140.

2. Görnandt, A.: Private communication, (2001).

3. Hilczer, B.; Malecki, J.: Electrets. Elseiver, New York, (1986).

4. Rao, S.S.; Sunar, M.: Piezoelectricity and its use in disturbance sensing and control of flexible structures: a survey. Applied Mechanics Review, 47, (1994), 113-123.

5. Shang, F.; Kuna, M.; Scherzer, M.: Analytical solutions for two penny-shaped crack problems in thermopiezoelectric materials and their finite element comparisons. submitted to International Journal of Fracture, (2001).

6. Tauchert, T.R.: Plane piezothermoelastic response of a hybrid laminate – a benchmark problem. Composite Structures, 39, (1997), 329-336.

7. Tzou, H.S.; Tseng, C.I.: Distributed piezoelectric sensor/actuator design for dynamic measurement/control of distributed parameter systems. a piezoelectric finite element approach. Journal of Sound and Vibration, 137, (1990), 1-18.

8. Tzou, H.S.; Ye, R.: Piezothermoelasticity and precision control of piezoelectric systems: theory and finite element analysis. Journal of Vibration and Acoustic, 116, (1994), 489-495.

Address: Dr. Fulin Shang, Prof. Dr. Meinhard Kuna and Dr. Matthias Scherzer, Institut für Mechanik und Fluiddynamik, TU Bergakademie Freiberg, Lampadiustrasse 4, D-09596 Freiberg, Germany. e-mail: meinhard.kuna@imfd.tu-freiberg.de